

OPEN

Circular RNA differential expression in blood cell populations and exploration of circRNA deregulation in pediatric acute lymphoblastic leukemia

Enrico Gaffo¹, Elena Boldrin², Anna Dal Molin¹, Silvia Bresolin³, Annagiulia Bonizzato³, Luca Trentin³, Chiara Frasson³, Klaus-Michael Debatin², Lueder H. Meyer², Geertruij te Kronnie³ & Stefania Bortoluzzi⁴

Circular RNAs (circRNAs) are abundantly expressed in the haematopoietic compartment, but knowledge on their diversity among blood cell types is still limited. Nevertheless, emerging data indicate an array of circRNA functions exerted through interactions with other RNAs and proteins, by translation into peptides, and circRNA involvement as regulatory molecules in many biological processes and cancer mechanisms. Interestingly, the role of specific circRNAs in leukemogenesis has been disclosed by a few studies, mostly in acute myeloid leukemia. In this study, circRNA expression in B-cells, T-cells and monocytes of healthy subjects is described, including putative new circRNA genes. Expression comparison considered 6,228 circRNAs and highlighted cell population-specific expression and exon usage patterns. Differential expression has been confirmed by qRT-PCR for circRNAs specific of B-cells (circPAX5, circAFF3, circIL4R, and circSETBP1) or T-cells (circIKZF1, circTNIK, circTXK, and circFBXW7), and for circRNAs from intronic (circBCL2) and intergenic regions that were overexpressed in lymphocytes. Starting from this resource of circRNA expression in mature blood cell populations, targeted examination identified striking and generalized upregulated expression of circPAX5, circPVT1 and circHIPK3 in pediatric B-precursor acute lymphoblastic leukemia, and disclosed circRNAs with variable expression across cytogenetic subtypes.

Circular RNAs (circRNAs), transcripts in which a downstream splice donor site is covalently bound to an upstream acceptor site by backsplicing, were recently recognized as evolutionary conserved and particularly stable transcriptome elements expressed with cell type- and differentiation-specific patterns^{1,2}.

In the last few years, diverse functional roles of specific circRNAs were discovered, making them attractive biological molecules for both fundamental and cancer research³. By acting as microRNA (miRNA) sponges and competitive endogenous RNAs, circRNAs can indirectly regulate miRNA-target expression, ultimately controlling key miRNA-involving axes^{4,5}. CircRNAs can also interact with RNA-binding proteins⁶ and regulate cellular processes, as shown for circFOXO3, which controls cell cycle progression by binding p21 and CDK1⁷. Notably, translation of some circRNAs into peptides not encoded by linear transcripts was demonstrated^{8–10} and linked to circRNA function, clarifying for instance the role of circZNF609 in the regulation of myoblast differentiation⁹ and rhabdomyosarcoma progression¹¹.

CircRNAs are abundantly expressed in the haematopoietic compartment^{12,13}. Identification of “scrambled exons” not only in hyperdiploid B-cell acute lymphoblastic leukemia (B-ALL), but also in naïve B-cells, haematopoietic stem cells and neutrophils, showed that circRNAs are present both in normal and malignant

¹Department of Molecular Medicine, University of Padova, Padova, Italy. ²Department of Pediatrics and Adolescent Medicine, Ulm University Medical Center, Ulm, Germany. ³Department of Women’s and Children’s Health, University of Padova, Padova, Italy. ⁴CRIBI Biotechnology Center, University of Padova, Padova, Italy. Enrico Gaffo, Elena Boldrin, Geertruij te Kronnie and Stefania Bortoluzzi contributed equally. Correspondence and requests for materials should be addressed to S. Bortoluzzi (email: stefania.bortoluzzi@unipd.it)

haematopoietic cells¹⁴. Considering normal haematopoiesis, Maass and colleagues¹⁵ described ~3,700 circRNAs expressed in plasma, serum, neutrophils, and platelets. Interestingly, enrichment of circRNAs compared to the host gene linear isoforms was found in whole blood¹², platelets and red blood cells¹⁶. Moreover, a recent work on the expression of 489 circRNAs across the haematopoietic tree showed 102 circRNAs differentially expressed in different cell types and maturation stages¹⁷ and prompted further investigation on circRNA expression variation in blood cell populations.

CircRNA involvement in cancer mechanisms is a prosperous research field¹⁸. Reports of circRNA expression variation in acute myeloid leukemia¹⁹, together with the deregulation of circRNAs expressed from MLL and its fusion partners in MLL rearranged leukemia^{20,21}, pointed at a role of circRNAs in haematopoietic malignancies. Data on circRNA expression and function in lymphoid malignancies are still limited, but indicate participation of these molecules in the disease. CircPVT1 derives from *PVT1* gene, which resides close to *MYC* in 8q24, identified as a risk locus of many cancers including leukemia. The circular but not the linear transcript of *PVT1* has high expression specifically in acute lymphoblastic leukemia²². Dahl *et al.*²³ provided the first information on the circRNAome in malignancies of mature B-cells, mantle cell lymphoma and multiple myeloma. In T-cell lymphoblastic lymphoma high circLAMP1 expression was recently linked to modulation of cell growth and apoptosis by regulation of the miR-615-5p/DDR2 pathway²⁴.

This study aims at enriching the knowledge of circRNA expression variation in mature blood cell populations and contributing to the exploration of circRNA expression in acute lymphoblastic leukemia. Investigation of the circular transcriptome of B-cell, T-cell and monocyte populations, reconstructed from high-depth RNA-seq data, disclosed differential and cell type-specific circRNA expression and alternative circularization patterns. Starting from this resource, a targeted examination of a set of circRNAs identified deregulated expression in cytogenetic subtypes of pediatric B-cell precursor acute lymphoblastic leukemia (BCP-ALL).

Results

CircRNAomes of B-, T-cell and monocyte populations. CircRNA expression in B-, T-cell and monocyte populations of healthy donors was investigated using high-depth ribodepleted RNA-seq data of 12 samples, with 4 replicates for each population of cells sorted from peripheral blood mononuclear cells, PBMCs (GEO series ID: GSE110159; Supplementary Methods and Supplementary Table 1).

CircRNA quantification and annotation were provided by CirComPara²⁵, which combined 9 circRNA detection software tools (CIRI2²⁶ Findcirc²⁷; CIRCexplorer2²⁸ on BWA²⁹, STAR³⁰, Segemehl³¹ and TopHat2³² aligners; DCC³³; circRNA_finder³⁴; and Segemehl³¹) to obtain the most reliable backsplices. Indeed, shared output from two or more algorithms for circRNA detection has been demonstrated to reduce false positive predictions^{35,36}. CirComPara performs read pre-processing quality filters, such as adaptor trimming, read mean quality selection and filtering by read length. Moreover, CirComPara counts the linearly spliced reads aligned to the backsplice junctions of each circRNA to estimate the expression of linear transcripts expressed from the circRNA's host-gene. These values were combined with the backspliced read counts, which measure the circular expression, to compute the proportion of expression between the circular and linear isoforms (Circular to Linear expression Proportion, CLP; see Methods). Further, the CLP embeds the concept of circular to linear expression correlation, so that CLP variation across conditions conveys the rate of independence between a circRNA and its host-gene's linear expression³³.

Overall, 68,007 circRNAs from 10,148 individual genes were detected by at least two methods. As reported by Hansen *et al.*³⁶, the algorithms mostly agreed on highly expressed circRNAs, whereas those detected by only one algorithm had generally low read counts (Supplementary Fig. 1).

Further, a sub-set of 6,228 circRNAs (from 3,323 genes) showing expression in all biological replicates of at least one cell type was retrieved and referred to as “high confidence” (HC) circRNAs (Supplementary Table 2). Comparison of circRNAs reported in this study with the results of Nicolet *et al.*¹⁷ confirmed concordance for 83% of the 489 HC circRNAs retrieved in the previous study and disclosed 5,824 additional HC circRNAs that were not yet investigated for expression variation in blood cell populations (Supplementary Fig. 2A).

Of the 6,228 HC circRNAs, 5,970 and 5,821 were expressed in B- and T-cells, and 5,144 in monocytes (Fig. 1a). The majority of circRNAs (4,763; 80%) were detected in all three cell types, including ubiquitous circZNF609³⁷, circHIPK3³⁸ and novel circRNAs. New circRNAs (e.g. circPICALM) are likely to be specific for the haematopoietic compartment. CircRNAs shared by two cell types where mostly common between lymphocytes.

Unsupervised principal component analysis showed relatively small variation of circRNA expression profiles within replicates of the same cell population, and pointed at circRNAome differences that clearly discriminated the cell types (Fig. 1b).

Expression of 21 HC circRNAs was validated by RT-PCR in PBMCs of different healthy donors (Supplementary Table 3; Table 1; Fig. 1c). This validation included exonic circRNAs from 15 different genes, two alternative isoforms of *IKZF1* and of the male-specific *ZFY* from the Y chromosome, one circRNA (18:63280887-63281214:–) derived from circularization of 328 bp of the unique large *BCL2* intron, and one circRNA from a putative new gene (“intergenic”, see below). The circular structure of circRNAs was corroborated by the observed enrichment of circRNAs after RNase R treatment, and detected by qRT-PCR with divergent primers specific for the backsplice junction^{14,27}. Moreover, all predicted backsplice junctions were confirmed by Sanger sequencing.

Multiple circular isoforms and circRNAs from new genes. Nearly all circRNAs (99.4%) derived from annotated genes, prevalently with backsplice junctions overlapping known exons (98.9%). Of the 71 circRNAs with both ends in intronic regions, the most abundant ones included the lymphocyte-specific circBCL2, which was validated, circHLA-E, circRASSF3, and several circMBL1 isoforms.

Almost one half of the circRNA host genes expressed multiple (up to 20) circular isoforms each (Fig. 1d). Preferential backsplice junction usage and expression of one or few prevalent isoforms were observed. The highest numbers of isoforms were expressed in monocytes by *AGTPBP1* (20) and *PICALM* (15), and in lymphocytes by *UBAP2* (19) and *ATM* (17).

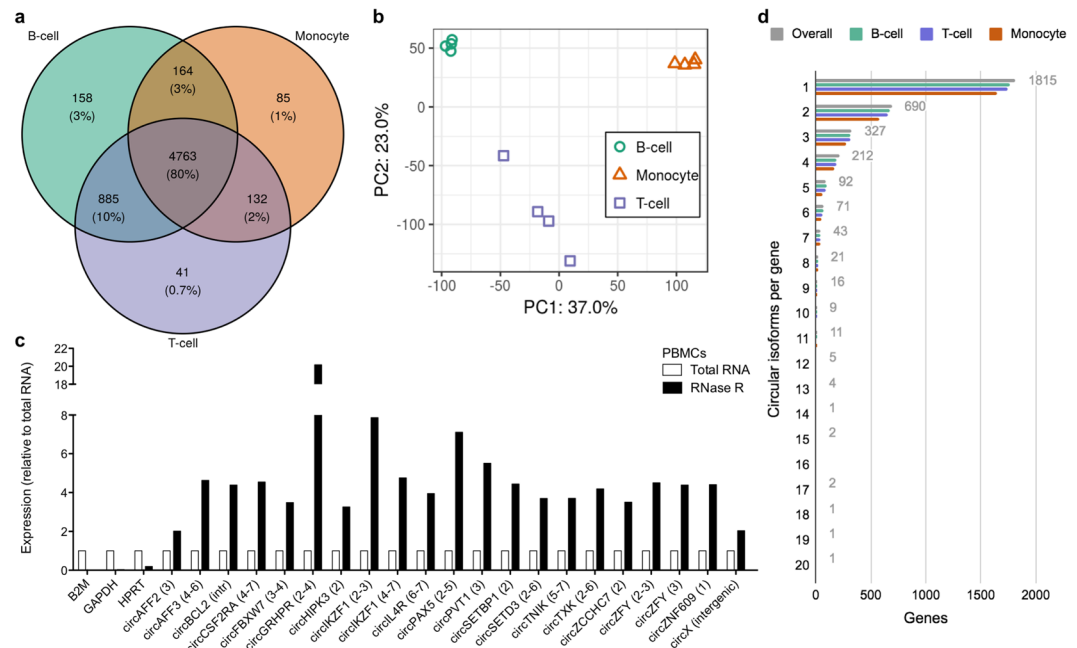


Figure 1. Comparison of circRNAome of B-, T-cells and monocytes. **(a)** Overlap of the 6,228 high confidence (HC) circRNAs expressed in B-, T-cells and monocytes; **(b)** Principal component analysis of HC circRNA expression profiles; **(c)** Validated circRNAs after RNase R treatment. B2M, GAPDH and HPRT mRNAs are shown as positive controls; Relative expression is calculated as $2^{-\Delta Cq}$, where ΔCq is the difference between RNase R treated and total PBMC RNA; **(d)** Number of circRNAs per gene expressed overall, and in each cell type.

Thirty-four circRNAs derived from intergenic regions. Intergenic circRNAs using the same backsplice ends in different combinations identified three loci expressing multiple isoforms. Five “intergenic” circRNAs derived from a putative new gene in the Xq11.2 region (chrX:65051462-65113813) (Supplementary Fig. 3). The most abundant circRNA of the locus, circX(intergenic) (X:65051462-65075912:+), previously detected in blood also by Memczak and colleagues¹², was validated (Fig. 1c).

Next, we investigated to what extent the expression is in favor of circular with respect to linear transcripts overlapping the backsplice junctions. CLP values range from 0 to 1: 0 comes when no circular expression is detected, $0 < CLP < 0.5$ represents circRNAs expressed less abundantly than the respective linear isoforms, 0.5 means that circular and linear transcripts have equivalent abundance, $0.5 < CLP \leq 1$ indicates circular isoforms expressed more abundantly than the respective linear transcripts. In particular, $CLP = 1$ when the linear expression relative to the circRNA is not detected. Interestingly, for 10 circRNAs no linear expression was detected. Moreover, the CLP was remarkably high (>0.95) for 14 circRNAs (Supplementary Table 4), including circGUSBP2 and circN-BPF10, with median CLP ranging from 0.99 to 1 in all cell populations (Supplementary Table 4), and circAFF2, which showed high CLP in monocytes (0.97). Preferential transcript circularization in mature blood cells of specific genes^{5,39} and/or higher stability of circular compared to linear RNAs^{16,40} could explain these findings.

Comparison between cell types disclosed cell type-specific circRNA expression and alternative circularization patterns.

Next, we aimed to define differences of the B-, T-cell and monocyte population circRNAomes. Pairwise comparisons of the three populations identified overall 1,369 significantly differentially expressed circRNAs (DECs) between cell types (Supplementary Table 5), which derived from 880 genes. Hierarchical clustering of DEC expression profiles reflected the sets of circRNAs upregulated in each cell type (Fig. 2a). DECs exclusively or over-expressed in one cell type indicated population-specific circRNAs (Fig. 2b): 622 were characteristic of B-cells, 183 of T-cells, and 438 of monocytes (1,243 in total; Supplementary Table 5). Moreover, 72 DECs were upregulated in both lymphocyte populations (Fig. 2b-d). No significantly enriched KEGG pathways of gene ontology terms resulted for genes of B-cell-characteristic circRNAs, which nevertheless, included genes involved in the B-cell receptor signalling pathway, such as SOS2 and NFKB1, or linked to B-cell functions. On the contrary, genes expressing T-cell characteristic circRNAs were significantly enriched the T-cell receptor signaling pathway. Moreover, genes of monocyte-characteristic circRNAs significantly enriched several biological processes and pathways related to monocyte functions. Other cell type-characteristic host-genes, instead, had cell functions not directly linked to the cell of origin (Supplementary Table 6).

Although cell type-characteristic circRNA sets were disjoint, the overlap of gene sets that expressed specific isoforms indicated alternative cell type-specific circularization patterns. Of note, 37 genes expressed circRNAs characteristic of two cell types and accounted for 14.7% of the genes with multiple cell type-specific circRNAs (Fig. 2c). Four circAKT3 isoforms showed cell type-specific expression, three for B- and one for T-cells; also four circMBNL1 were cell type-specific, 3 for B-cells and one for monocytes. Moreover, six different GRK3 circular isoforms were specifically overexpressed in B-cells, whereas two others were overexpressed only in monocytes.

CircRNA	Expression				qRT-PCR	Previous data	
	Reads			CircRNA		Locus	
	B	T	M				
circAFF2 (3) X:148661908–148662768:+	18	6	113	Upregulated in TCF3-PBX1 ALL	Downregulated in acute myeloid leukemia (AML) compared with healthy controls ⁷² ; Upregulated in monocytes ⁴⁷	Deletion of the locus associated with Fragile X syndrome ⁷³ ; Linear transcripts not expressed	
circAFF3 (4–6) 2:100006632–100008932–	93	0	5	Upregulated in B-cells and ALL	—	Involved in fusions with MLL in ALL ⁷⁴	
circBCL2 (intr) 18:63280887–63281214:–	36	40	0	Upregulated in lymphocytes and ETV6-RUNX1 ALL	—	Involved in frequent translocations in follicular lymphoma ⁷⁵	
circCSF2RA (4–7) X:1285778–1290509:+	1	0	186	—	—	Frequently deleted in BCP-ALL ⁷⁶ ; Linear transcripts not expressed	
circFBXW7 (3–4) 4:152411303–152412529:–	595	1145	334	Upregulated in T-cells and expressed in ALL	Tumor suppressor in glioma ⁴⁶ , clear cell renal cell carcinoma ⁷⁷ and breast cancer progression ⁷⁸ by miRNA sponging and protein coding potential.	Mutated or deleted in T-ALL ⁷⁹ ; Circular isoform higher than the linear form ⁸⁰	
circGRHPR (2–4) 9:37424845–37426654:+	90	50	23	—	Validated in ¹⁰	Involved in fusions with BCL6 in some lymphomas ⁸¹	
circHIPK3 (2) 11:33286413–33287511:+	151	187	553	Upregulated in monocytes and ALL	Oncogenic in different cancer types ⁴³	Circular isoform more abundant than the linear one ³⁸	
circIKZF1 (2–3) 7:50319048–50327757:+	77	211	30	Downregulated in T-cells, and in BCR-ABL1, hyperdiploid ALL	—	Deleted or mutated in ALL ⁸²	
circIKZF1 (4–7) 7:50376533–50391863:+	11	20	13	—	—	—	
circIL4R (6–7) 16:27346467–27352696:+	154	13	0	Upregulated in B-cells, Downregulated in ALL	Deregulated expression in hepatocellular carcinoma ⁴⁷	Frequently mutated in primary mediastinal large B-cell lymphoma ⁸³	
circPAX5 (2–5) 9:37002648–37020801:–	34	0	0	Upregulated in B-cells and ALL	—	Involved in translocations or deletions in haematologic malignancies ⁴¹	
circPVT1 (3) 8:127890589–127890998:+	18	20	3	Upregulated in ALL	Oncogenic in different cancer types ⁴⁸ , Upregulated and oncogenic in ALL ²²	Oncogenic long non-coding RNA ⁸⁴ , Upregulated and oncogenic in T-ALL ⁸⁵	
circSETBP1 (2) 18:44701175–44701832:+	136	13	5	Upregulated in B-cells and hyperdiploid ALL	—	Somatic mutations in myeloid leukemia ⁸⁶	
circSETD3 (2–6) 14:99458279–99465813:–	201	367	402	—	Not binding to Argonaute ¹⁰ , Downregulated in colorectal cancer ⁸⁷ , Tumor suppressor in hepatocellular carcinoma, sponge for microRNA-421 ⁸⁸	Amplification (14q32) in AML ⁸⁹ ; Linear transcripts not expressed	
circTNIK (5–7) 3:171188702–171194635:–	0	43	0	Upregulated in T-cells	Upregulated in quadriceps femoris muscle of myotonic dystrophy ⁹⁰	—	
circTXK (2–6) 4:48104901–48114402:–	1	72	0	Upregulated in T-cells	—	—	
circZCCHC7 (2) 9:37126312–37126942:+	1048	385	94	Upregulated in B-cells, Downregulated in ALL	Associated with polysomes ¹⁰ ; Validated in ¹⁰	Downregulated in relapsed ALL ⁹¹ Linear transcripts not expressed	
circZFY (2–3) Y:2953909–2961646:+	70	106	50	Upregulated in ALL	Validated in ³⁸ , Increased in tuberculosis patients ⁹²	—	
circZFY (3) Y:2961074–2961646:+	48	97	48	—	—	—	
circZNF609 (1) 15:64499293–64500166:+	254	743	285	—	Roles in Hirschsprung disease (ceRNA) ³⁷ , and in myoblast proliferation (protein coding) ⁹ ; Validated in ³⁷	—	
circX (intergenic) X:65051462–65075912:+	214	294	3	Upregulated in lymphocytes, Downregulated in ALL	—	—	

Table 1. Summary of validated circRNAs. Twenty-one circRNAs were validated by RT-PCR in PBMCs of healthy donors and all were resistant to RNase R treatment. CircRNA names include the gene locus, the exons involved in the backsplicing and the genomic coordinates. Expression (Reads) is indicated as the average read count of the four biological replicates per each cell type (B, B-cell; T, T-cell; M, monocyte). Expression (qRT-PCR) indicates circRNAs for which expression in blood cell populations and in BCP-ALL was screened by qRT-PCR. Previous data provide information about the circRNA and/or the locus from the literature.

Quantification by qRT-PCR in B-cells, T-cells and monocytes sorted from 5 independent healthy donors confirmed RNA-seq results for all 15 tested circRNAs, supporting data robustness and reproducibility (Fig. 2d and Supplementary Fig. 4).

Significant up-regulation in B-cells of 5 circRNAs, including circAFF3 (exons 4–6), circIL4R (exons 6–7), circSETBP1 (exon 2) was confirmed. Moreover, high circRNA expression from the genomic region 9p13.2 including PAX5 (Supplementary Fig. 5) was validated: circPAX5 (exons 2–5) and circZCCHC7 (exon 2) were both B-cell-specific, while a trend toward upregulation of circGRHPR in B-cells was in agreement with the estimate from the RNA-seq data. PAX5 exerts a striking role in the commitment of B-cells⁴¹ and co-expression of PAX5 and ZCCHC7 linear transcripts was described during the progression from common lymphocyte precursors to pre-pro-B cells⁴². Suggestive of co-regulation of the 9p13.2 locus, circPAX5, circZCCHC7 and circGRHPR isoforms were all overexpressed specifically in B-cells. CircPAX5 and circZCCHC7 were previously detected in

CD19+ cells¹⁴. Both circZCCHC7 and circGRHPR were identified in CD34+ cells and, according to data on RNA base modification promoting efficient initiation of protein translation from circRNAs in human cells, are likely to encode peptides¹⁰.

Regarding T-cells, significant overexpression was confirmed for circIKZF1 (exons 2–3), circTNIK (exons 5–7), circTXK (exons 2–6) and, in agreement with previous reports¹⁷, for circFBXW7 (exons 3–4). Also an increasing trend for circZFY (exons 2–3) in T-cells and for circAFF2 (exon 3) in monocytes, in agreement with Nicolet *et al.*¹⁷, confirmed RNA-seq results, while significant upregulation of circX(intergenic) and circBCL2(intronic) in lymphocytes and of circHIPK3 (exon 2) in monocytes was validated.

Nicolet *et al.*¹⁷ found 102 circRNAs differentially expressed across blood cell types and stages, 98 of which were detected in our data. In particular, 42 circRNAs resulted differentially expressed also in our comparison, 31 of which were cell type-specific. Overall, our data were in agreement with circRNA clusters previously associated to mature cell populations (Supplementary Fig. 2b). CircRNAs previously assigned to lymphoid cell-specific clusters showed the highest expression in B-cells or T-cells, including circZCCHC7 and circFBXW7 that we experimentally validated. Nine out of 10 circRNAs previously deemed as monocyte-specific were recalled by our analysis being more expressed in monocytes, including circAFF2. However, the majority of the 1,243 circRNAs defined as cell type-specific in the present study, including 11 out of 15 circRNAs for which cell type-specific overexpression was confirmed by qRT-PCR in this study (Fig. 2d), were not represented in the clusters defined by Nicolet *et al.*

Next, we inspected whether the abundance of circular isoforms with respect to linear expression was altered between the cell types. CLP variations across sample conditions indicate the rate of independence between a circRNA and the host-gene linear expression. First, we observed that the number of circRNAs with more abundant circular expression proportion (CLP > 0.5) was highest in lymphoid cells (185 in monocytes, 333 and 364 in B-cells and T-cells, respectively), which is in accordance with previous observations on a smaller set of circRNAs¹⁷. Then, we identified 687 circRNAs (from 495 genes) with host-gene independent expression (Supplementary Table 7). Among DECIs, 163 had significant variation of circular expression proportion between cell types in agreement to the differential absolute expression, indicating that observed variations of these circRNA expression level across cell populations are not due to a corresponding variation of linear expression. CircIKZF1, for which upregulation in T-cells was validated, was also expressed with high CLP in T-cells. In particular, 25 circRNAs showed high and significantly varied circular expression proportion (Supplementary Fig. 6), including the validated circX(intergenic) and three additional intergenic circRNAs, all overexpressed in B- and T-cells. CircSMARCA5 had the highest absolute and relative circular expression in B-cells, while it was significantly lower in T-cell and lowest in monocytes (Supplementary Fig. 7).

Expression of circRNAs in six cytogenetic subtypes of B-cell precursor acute lymphoblastic leukemia.

Starting from the above described transcriptome-wide circRNA resource, the expression and possible deregulation of circRNAs in BCP-ALL was examined for a target set of circRNAs. The selected circRNAs showed lymphocyte specificity and/or derived from leukemia-associated loci. Following these criteria, ten of the circRNAs with validated upregulation in B-cells, T-cells or in both lymphocyte populations (Fig. 2d) were selected for quantification in BCP-ALL, including circRNAs from known genes (*AFF2*, *AFF3*, *BCL2*, *FBXW7*, *IKZF1*, *IL4R*, *PAX5*, *SETBP1* and *ZCCHC7*) and the newly identified circX(intergenic) highly expressed in lymphocytes. In addition, circZFY, a circRNA expressed at a high level in blood cells of male subjects; circHIPK3, for which oncogenic properties are known in solid cancers⁴³; and circPVT1, recently linked to acute lymphoblastic leukemia²², were included.

Expression of the 13 selected circRNAs was measured by qRT-PCR in 32 BCP-ALL patient-derived xenograft (PDX) samples (Supplementary Table 8).

All leukemic samples together were first compared with B-cells from healthy donors (Supplementary Fig. 8 and Fig. 3a) to check for deregulated circRNA expression in leukemic cells. For seven circRNAs the expression was significantly different in ALL samples compared with B-cells. CircIL4R, circZCCHC7 and circX(intergenic), all highly expressed in lymphocytes, were less expressed in ALL. Conversely, overexpression of circAFF3, circHIPK3, circPVT1 and circPAX5 in BCP-ALL emerged. Differently from circPVT1 and circHIPK3, a functional characterization of circPAX5 and circAFF3 is still lacking. Thus, custom functional predictions, in terms of possible miRNA-binding sites, RNA binding protein (RBP) binding sites, and coding potential were obtained (Fig. 3b and Supplementary Fig. 9).

Further, we explored expression of the target set of circRNAs across the main BCP-ALL cytogenetic subtypes (Fig. 3a). Cytogenetic subtypes are characterized by specific genetic lesions, including recurrent translocations (*MLL* rearrangements, *BCR/ABL*, *ETV6-RUNX1*, and *TCF3-PBX1* fusions) and hyperdiploid karyotype. Cytogenetic subtype characterization is instrumental for risk prognosis and treatment stratification of leukemia patients. Leukemic cells of different subtypes have distinct biological features, gene expression profiles and specific miRNA signatures^{44,45}. In this context, novel information about the heterogeneous nature of acute leukemias was added by the observed significant circRNA expression differences among cytogenetic subtypes (Fig. 3a). CircAFF2 was highly expressed in *TCF3-PBX1* BCP-ALL and, to a lesser extent, in *ETV6-RUNX1* BCP-ALL, compared to B-cells and other cytogenetic BCP-ALL subgroups. CircBCL2(intronic) was upregulated in ALL with *ETV6-RUNX1* fusions. CircSETBP1 and circX(intergenic) were both very reduced in *MLL* rearranged samples. CircIKZF1 was lower in *BCR-ABL* and hyperdiploid leukemias compared with the *ETV6-RUNX1* subtype, in which the expression was conserved at levels comparable with B-cells.

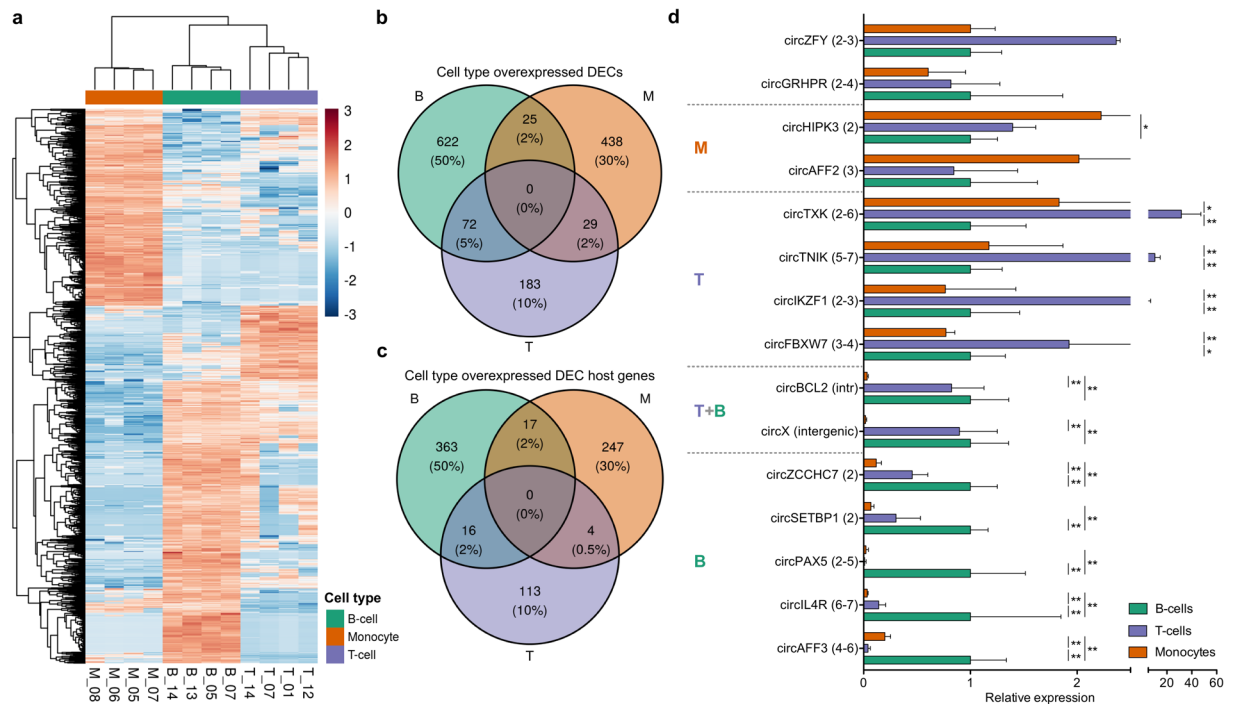


Figure 2. Differential expression of circRNAs in mature blood cell populations. **(a)** Hierarchical clustering (Euclidean distance; complete clustering) of expression profile of 1,369 significantly differentially expressed circRNAs (DECs) between cell types. **(b)** Venn diagram showing the overlap of circRNAs overexpressed in each population: non-intersection portions outline cell type-specific overexpressed circRNAs. **(c)** Host genes for DECs overexpressed only in one cell type: intersection regions represent genes expressing different circular isoforms overexpressed in different cell types. **(d)** qRT-PCR validation of expression of 15 circRNAs, 13 of which are significantly overexpressed in monocytes (M), T-cells (T), B-cells (B) or both lymphocyte populations (T + B). In agreement with RNA-seq data, circZFY and circGRHPR were not significantly differentially expressed. Gene exons involved in the backsplice are displayed in parentheses after the circRNA name. Expression relative to the mean of B-cells. Mann-Whitney U-test, p-value * < 0.05, ** < 0.01.

Discussion

This study disclosed the circRNAomes of B-, T-cell and monocyte populations, first providing a large catalogue of circRNAs expressed in normal B-, T-cell and monocytes. Comparison of the cell population circRNA expression profiles confirmed previous findings on variable circRNA expression among different blood cells¹⁷ and further suggested hundreds of circRNAs with cell type-specific expression. Moreover, complex patterns of cell type-specific alternative circularization were disclosed. These results were backed up by qRT-PCR validations in independent samples for selected circRNAs.

We speculate that at least some of the circRNAs with high cell type-specific expression could be involved in the regulation or maintenance of the specific cell functions. Functional data were available only for a few of the circRNAs that we validated for specific overexpression, and when available, they were often from a different context (Table 1). For instance, circFBXW7, overexpressed in T-cells, was shown to suppress cancerogenesis and malignant progression in solid tumors, and to encode a 185 amino acids functional peptide⁴⁶. Besides, circZCCHC7, highly expressed in lymphocytes, was shown to be associated to polysomes in 293 and HeLa cells¹⁰. Therefore, further functional experiments, like circRNA overexpression or knockdown, will be required to elucidate the role of specific circRNAs in normal haematopoiesis.

In a prospective view toward understanding translational relevance of our findings, the second part of the study reported deregulation of circRNAs in BCP-ALL disclosed by screening of a target set of circRNAs in six cytogenetic subtypes. Considering circRNAs downregulated in BCP-ALL, circIL4R showed deregulated expression also in hepatocellular carcinoma⁴⁷. CircX(intergenic), highly expressed in lymphocytes and less expressed in ALL, could derive from an unannotated gene that produces only circularized transcripts.

Moreover, four circRNAs were markedly upregulated in BCP-ALL: circPVT1, circHIPK3, circPAX5 and circAFF3. Observed circPVT1 upregulation in pediatric BCP-ALL is in line with previous reports of various cancer types⁴⁸ including ALL²². CircPVT1, originating from a cancer susceptibility locus including the oncofetal lncRNA PVT1 and MYC, was first detected in gastric cancer, where upregulation promotes cell proliferation by sponging members of the miR-125 family⁴⁹. As recently reviewed^{48,50}, functional studies showed circPVT1 oncogenic properties in solid tumours: circPVT1 sponges different tumour suppressor miRNAs and hence derepresses expression of oncogenic proteins, ultimately promoting tumor-associated phenotypes like proliferation, invasion, angiogenesis and drug resistance. Plus, circPVT1 levels significantly impact drug response in multiple myeloma⁵¹ highlighting its therapeutic potential. CircPVT1, but not PVT1 linear transcript, was shown to be upregulated

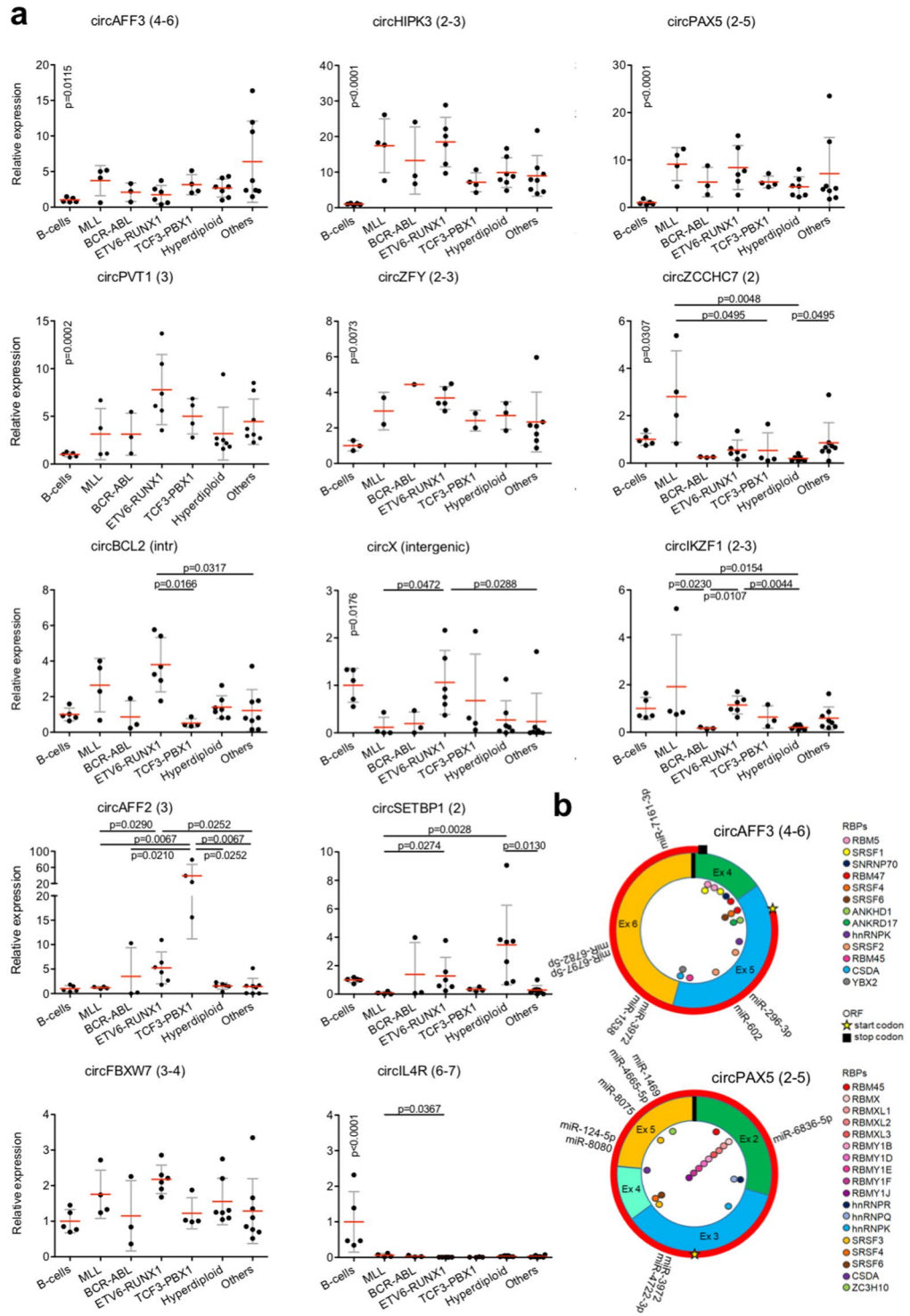


Figure 3. CircRNA expression in patient-derived BCP-ALL samples and predicted functions of circAFF3 and circPAX5. **(a)** Relative expression of 12 circRNAs assessed by qRT-PCR in healthy PBMC derived B-cells and 32 BCP-ALL patient-derived xenograft samples with different genetic subtypes: MLL rearranged ($n = 4$), BCR-ABL (3), ETV6-RUNX1 (6), TCF3-PBX1 (4), high hyperdiploid (>50 chromosomes, 7), “Others” (negative for the mentioned rearrangements, 8). Expression relative to B-cells. Only significant p-values (<0.05) are indicated (Kruskal-Wallis test, corrected for multiple testing with Benjamini, Krieger and Yekutieli procedure). P-values on “B-cells” refer to B-cells vs all BCP-ALL samples (Mann Whitney U-test, only significant values shown). **(b)** Prediction of functions and interactions of circAFF3 and circPAX5, including predicted miRNA-binding sites, sequence motifs possibly recognized by RNA binding proteins (RB) and open reading frames (ORFs) of at least 150 nt spanning the backsplice.

in bone marrow of adult ALL patients²². Knockdown of circPVT1 in B- and T-ALL cell lines arrested cell growth and induced apoptosis through inhibition of c-Myc and Bcl-2 expression mediated by sponging of miR-125 and miR-let7. Recently, Tashiro *et al.*⁵² reported the potency of circPVT1 to encode a protein of 140 amino acids. Our data are the first observation of a general upregulation of circPVT1 in specimens of pediatric patients with BCP-ALL. In non-small cell lung cancer, Qin *et al.*⁵³ showed that circPVT1 regulates Bcl-2 expression by sponging miR-497. The tumour suppressor role of miR-497 in cancer entities, including BCP-ALL⁵⁴ advocates mechanistic investigation of the circPVT1-miR-497 axis in these leukemias.

CircHIPK3 is a conserved and highly expressed circRNA. Previous studies showed a cytoplasmic location for circHIPK3 and indicated that it is unlikely to be translated, albeit containing the canonical AUG of the associated linear transcripts³⁸. CircHIPK3 upregulation was reported in various solid cancers and linked to the reduction of the suppressive activity of several miRNAs⁴³, with potential functional implications. CircHIPK3 binding to miR-124 was indeed able to restore expression of miRNA targets sustaining cell proliferation in lung cancer and hepatocellular carcinoma^{55,56}. In light of available data, upregulation of circHIPK3 could influence the growth of leukemic cells as well.

The upregulation of circPAX5 in leukemic cells is a new finding, which is worth investigating further to clarify if circPAX5 plays a role in normal haematopoiesis, and explore possible involvement in the disease mechanism. The circPAX5 specific expression in B-cells could point at a cooperating role with the linear transcript that codes for a key B-lineage transcription factor. Predicted binding sites for miRNAs on circPAX5 (Fig. 3b and Supplementary Fig. 9) included miR-124, for which circHIPK3 acts as a sponge^{55,56}, and suggested a possible synergy of circRNAs upregulated in leukemic cells. CircPAX5 presented a translation start site in exon 3 without stop codons afterwards to interrupt the ORF spanning the backsplicing.

Expression of the B-cell specific circAFF3 increased around four times in BCP-ALL. CircAFF3 has putative recognition motifs for several miRNAs, including miR-296-5p, an antimetastatic miRNA whose sequestration by another circRNA was previously linked to cancer^{57,58}. In addition, multiple putative binding sites for members of the serine/arginine-rich splicing factor family linked to leukemogenesis⁵⁸, and a 215 aa ORF were predicted for circAFF3 (Fig. 3b and Supplementary Fig. 9).

In conclusion, our data advanced the knowledge of the circular transcriptome in normal hematopoiesis and, besides encouraging future in depth investigation of circRNAs in even more defined sub-populations and blood cell differentiation and maturation stages, may be useful for mechanistic studies of circRNAs in blood cell biology. CircRNA deregulation in patient-derived BCP-ALL samples disclosed by our targeted analysis definitely advocates a multi modal strategy of leukemia transcriptome investigation that integrates linear, circular and miRNAs, instructing also functional investigation of specific circRNAs.

Methods

Sample collection, cell sorting and sequencing. Mononuclear cells (PBMCs) were isolated from peripheral blood of healthy adult donors (Department of Transfusional Medicine, University Hospital of Padova; Supplementary Table 1) with LymphoprepTM density gradient centrifugation (STEMCELL Technologies, Vancouver, BC, Canada) followed by haemolysis (0.5 M EDTA pH 8.0). CD45+ (ECD conjugated, Beckman Coulter, Indianapolis, USA) population from PBMCs was separated by sorting with FACS AriaTM III (Becton Dickinson, NJ07417, USA) into B-cells, T-cells and monocytes, after labeling with anti CD19 (clone J4.119, PE-Cy7 conjugated, Beckman Coulter, Indianapolis, USA), CD3 (clone SK7, APC Cy7 conjugated, Becton Dickinson, San Jose, CA, CD14 antibodies) and CD14 (clone RM052, PE conjugated, Beckman Coulter, Indianapolis, USA), respectively. For each cell type, four biological replicates were obtained from different donors.

Total RNA was extracted with TRIzol reagent (Thermo Fisher Scientific, Waltham, Massachusetts) and precipitated with isopropanol. All samples showed a RNA integrity number (RIN) > 7, assessed with Agilent 2100 Bioanalyzer (Santa Clara, CA, USA). RNA libraries were prepared with the TruSeq Stranded Total RNA Ribo-Zero Gold kit. Paired-end reads 100–125 bp long were sequenced with an Illumina[®] HiSeq2000 (San Diego, CA, USA) at an average sequencing depth of 147 million reads per sample (8 453.25 million bases; Supplementary Table 1). All experiments involving human material followed the principles outlined in the Helsinki Declaration of 1964, as revised in 2000, and informed consent has been obtained for all the participants. The study has been approved by the ethics committee of Padova University Hospital and written informed consent was obtained from all subjects.

CircRNA detection and quantification. The analysis was based on the Ensembl GRCh38 human genome and annotation v87.

CircRNAs were detected and quantified by CirComPara v0.6²⁵ using 9 backsplice detection methods (CIRI2 v2.0.2²⁶ Findcirc v1.2²⁷; CIRCexplorer2 v2.3.3²⁸ combined to each of BWA²⁹, STAR³⁰, Segemehl³¹ and TopHat2³² alignments; DCC v0.4.6³³; circRNA_finder v1.1³⁴; and Segemehl v0.3.4) and default parameters, which selected only the circRNAs detected by two or more methods.

Version of other software tools included in CirComPara: Bowtie2 v2.2.9⁵⁹, BWA v0.7.15-r1140²⁹, STAR v2.6.1d³⁰, Segemehl v0.3.4³¹, and TopHat2 v2.1.0³² with Bowtie v1.1.2⁶⁰.

CirComPara preprocessed raw reads with Trimmomatic v0.38⁶¹ to remove residual adapters and select reads by quality and length. Read linear mapping to the human genome was performed with HISAT2 v2.0.4⁶².

CirComPara implements circular to linear ratio as described in³³.

CirComPara's non-default parameters used for analyses: Adapter sequence = Trimmomatic file TruSeq3-PE.fa; PREPROCESSOR = Trimmomatic, TOGGLE_TRANSCRIPTOME_RECONSTRUCTION = 'False', LIN_COUNTER = 'ccp', CIRCRNA_METHODS = "testrealign, dcc, ciri, circexplorer2_star, findcirc, circexplorer2_segemehl, circexplorer2_bwa, circexplorer2_tophat, circrna_finder"; PREPROCESSOR_PARAMS = "MAXINFO:40:0.5

LEADING:20 TRAILING:20 SLIDINGWINDOW:4:30 MINLEN:50 AVGQUAL:30"; HISAT2_EXTRA_PARAMS = "-rna-strandness RF"; BWA_PARAMS = ["-T", "19", "-c", "1"]; SEGEMehl_PARAMS = ["-M", "1", "-D", "0"]; TOPHAT_PARAMS = ["-zpacker", "pigz", "-max-multihits", "1"]; STAR_PARAMS = ["-outFilterMultimapNmax", "1", "-outSJfilterOverhangMin", "15", "15", "15", "15", "-alignSJoverhangMin", "15", "-alignSJDBoverhangMin", "15", "-seedSearchStartLmax", "30", "-outFilterScoreMin", "1", "-outFilterMatchNmin", "1", "-outFilterMismatchNmax", "2", "-chimSegmentMin", "15", "-chimScoreMin", "15", "-chimScoreSeparation", "10", "-chimJunctionOverhangMin", "15"]; MIN_READS = 2; MIN_METHODS = 2; DCC_EXTRA_PARAMS = ["-fg", "-M", "-F", "-Nr", "1", "1"]; TESTREALIGN_PARAMS = ["-q", "median_30"]; FINDCIRC_EXTRA_PARAMS = ["-best-qual", "40"]; FIX_READ_HEADER = "True".

Differential expression. Differential expression in pairwise comparisons between the three cell types was assessed by DESeq2⁶³ (v1.22.2) with local fit, model including sex factor, fold change shrinkage, Wald significance tests, no independent filtering and *poscounts* normalization. P-values were corrected for multiple tests with the Benjamini Hochberg procedure considering at once all the tests performed in all the contrasts. Adjusted p-values ≤ 0.05 were chosen to select the significantly differentially expressed circRNAs.

CircRNA to host-gene linear expression variation was assessed using CircTest³³ v0.1.1 and selecting adjusted p-values ≤ 0.05 .

Circular to linear expression proportion (CLP) for each circRNA was computed as in³³:

$$CLP = \frac{\text{circular reads}}{\text{circular reads} + \text{linear reads}}$$

Graphics were generated with the ggplot2 v3.1.0, pheatmap v1.0.12, VennDiagram⁶⁴ v1.6.20, and data.table v1.11.8 R packages.

Experimental validations. Validation of 21 circRNAs was performed on pooled total or RNase R treated RNA of PBMCs from 4 healthy donors to test resistance to RNase R treatment. For 15 of the validated circRNAs qRT-PCR quantification in B-cells, T-cells and monocytes from 5 healthy donors, isolated as described above, was obtained. Moreover, 13 circRNAs were quantified in patient-derived xenograft samples of pediatric BCP-ALL obtained as previously described⁶⁵.

Leukemia samples were obtained from pediatric BCP-ALL patients at diagnosis or relapse upon informed consent of patients and/or their legal guardians in accordance with the institution's ethical review boards. All animal experiments were approved by the appropriate authority (Regierungspräsidium Tübingen) and carried out following the national animal welfare guidelines.

Total RNA was isolated by TRIzolTM (Thermo Fisher Scientific) extraction, followed by isopropanol precipitation. PBMC RNA was treated with 4 u RNase R/ μ g (Epicentre) at 37 °C for 15 min and with 5 μ l of DNase I (Zymo Research) at room temperature for 15 min. RNA was then purified with RNA Clean & ConcentratorTM -5 (Zymo Research) and quantified with Nanodrop. Reverse Transcription was performed from 500 ng RNA with SuperScriptII (Thermo Fisher Scientific), with random primers (Thermo Fisher Scientific). Divergent primers (Supplementary Table 3) for selective amplification of circRNAs were designed with Primer3 v. 0.4.0^{66,67}. RT-PCR was performed from 12.5 ng cDNA with Taq DNA Polymerase (Qiagen) with the following protocol. Initial denaturation: 95 °C for 15 min; 35 cycles: 95 °C for 30 sec, 54–60 °C for 30 sec, 72 °C for 30 sec; final extension: 72 °C for 10 min. Sanger Sequencing was performed on PCR products after cleaning with Wizard[®] SV Gel and PCR Clean-Up System (Promega), by Eurofins Genomics.

qRT-PCR was performed with technical triplicates with SsoAdvanced Universal SYBR Green Supermix (BioRad) in 10 μ l per well, from 5 ng cDNA, 500 nM primers. The reaction was incubated in CFX Connect Real-Time PCR Detection System (BioRad) with the following protocol: 95 °C for 30 sec; 40 cycles: 95 °C for 5 sec, 58 °C for 30 sec. C_q were calculated with CFX MaestroTM Software (BioRad). Relative expression is expressed as $2^{-\Delta C_q}$ (sample)/average $2^{-\Delta C_q}$ (B-cells), where $\Delta C_q = C_q$ (target gene) - C_q (reference gene: B2M). B2M was chosen with NormFinder⁶⁸ as reference gene among three tested (B2M, GAPDH, HPRT).

Statistical significance of differential expression was calculated for comparisons between B-cells, T-cells and monocytes and BCP-ALL vs B-cells with Mann Whitney U-test; for multiple comparison of different genetic subgroups with Kruskal-Wallis test, corrected with the Benjamini, Krieger and Yekutieli procedure. Tests were performed with Prism v7 (GraphPad).

Functional predictions. Putative circAFF3 and circPAX5 sequences were assembled joining annotated exons comprised in the genomic coordinates corresponding to the validated backsplice ends.

MiRNA binding sites were predicted using miRanda⁶⁹, and only target sites with a score in the highest 10% and energy in the lower 10% were considered. Recognition motifs for RNA binding proteins were predicted using beRBP⁷⁰, keeping only sequence motifs with voteFrac score in highest 10%.

Open reading frames of at least 150 nt were predicted using ORFfinder⁷¹ further keeping only the longest ORF spanning the backsplice.

References

- Rybak-Wolf, A. *et al.* Circular RNAs in the Mammalian Brain Are Highly Abundant, Conserved, and Dynamically Expressed. *Mol. Cell* **58**, 870–885 (2015).
- Salzman, J., Chen, R. E., Olsen, M. N., Wang, P. L. & Brown, P. O. Cell-type specific features of circular RNA expression. *PLoS Genet.* **9**, e1003777 (2013).
- Kristensen, L. S., Hansen, T. B., Venø, M. T. & Kjems, J. Circular RNAs in cancer: opportunities and challenges in the field. *Oncogene* **37**, 555–565 (2018).

4. Li, F. *et al.* Circular RNA ITCH has inhibitory effect on ESCC by suppressing the Wnt/ β -catenin pathway. *Oncotarget* **6**, 6001–6013 (2015).
5. Hansen, T. B. *et al.* Natural RNA circles function as efficient microRNA sponges. *Nature* **495**, 384–388 (2013).
6. Schneider, T. *et al.* CircRNA-protein complexes: IMP3 protein component defines subfamily of circRNPs. *Sci. Rep.* **6**, 31313 (2016).
7. Du, W. W. *et al.* Foxo3 circular RNA retards cell cycle progression via forming ternary complexes with p21 and CDK2. *Nucleic Acids Res.* **44**, 2846–2858 (2016).
8. Pamudurti, N. R. *et al.* Translation of CircRNAs. *Mol. Cell* **66**, 9–21.e7 (2017).
9. Legnini, I. *et al.* Circ-ZNF609 Is a Circular RNA that Can Be Translated and Functions in Myogenesis. *Mol. Cell* **66**, 22–37.e9 (2017).
10. Yang, Y. *et al.* Extensive translation of circular RNAs driven by N⁶-methyladenosine. *Cell Res.* **27**, 626–641 (2017).
11. Rossi, F. *et al.* Circ-ZNF609 regulates G1-S progression in rhabdomyosarcoma. *Oncogene*, <https://doi.org/10.1038/s41388-019-0699-4> (2019).
12. Memczak, S., Papavasileiou, P., Peters, O. & Rajewsky, N. Identification and Characterization of Circular RNAs As a New Class of Putative Biomarkers in Human Blood. *PLoS One* **10**, e0141214 (2015).
13. Bonizzato, A., Gaffo, E., Te Kronnie, G. & Bortoluzzi, S. CircRNAs in hematopoiesis and hematological malignancies. *Blood Cancer J.* **6**, e483 (2016).
14. Salzman, J., Gawad, C., Wang, P. L., Lacayo, N. & Brown, P. O. Circular RNAs are the predominant transcript isoform from hundreds of human genes in diverse cell types. *PLoS One* **7**, e30733 (2012).
15. Maass, P. G. *et al.* A map of human circular RNAs in clinically relevant tissues. *J. Mol. Med.* **95**, 1179–1189 (2017).
16. Alhasan, A. A. *et al.* Circular RNA enrichment in platelets is a signature of transcriptome degradation. *Blood* **127**, e1–e11 (2016).
17. Nicolet, B. P. *et al.* Circular RNA expression in human hematopoietic cells is widespread and cell-type specific. *Nucleic Acids Res.* **46**, 8168–8180 (2018).
18. Ng, W. L., Mohd Mohidin, T. B. & Shukla, K. Functional role of circular RNAs in cancer development and progression. *RNA Biol.* **15**, 995–1005 (2018).
19. Hirsch, S. *et al.* Circular RNAs of the nucleophosmin (NPM1) gene in acute myeloid leukemia. *Haematologica*, <https://doi.org/10.3324/haematol.2017.172866> (2017).
20. Guarnerio, J. *et al.* Oncogenic Role of Fusion-circRNAs Derived from Cancer-Associated Chromosomal Translocations. *Cell* **166**, 1055–1056 (2016).
21. Molin, A. D. *et al.* CircRNAs Are Here to Stay: A Perspective on the MLL Recombinome. *Frontiers in Genetics* **10** (2019).
22. Hu, J. *et al.* Circular RNA PVT1 expression and its roles in acute lymphoblastic leukemia. *Epigenomics* **10**, 723–732 (2018).
23. Dahl, M. *et al.* Enzyme-free digital counting of endogenous circular RNA molecules in B-cell malignancies. *Lab. Invest.* **98**, 1657–1669 (2018).
24. Deng, L. *et al.* Circ-LAMP1 promotes T-cell lymphoblastic lymphoma progression via acting as a ceRNA for miR-615-5p to regulate DDR2 expression. *Gene* **701**, 146–151 (2019).
25. Gaffo, E., Bonizzato, A., Kronnie, G. & Bortoluzzi, S. CirComPara: A Multi-Method Comparative Bioinformatics Pipeline to Detect and Study circRNAs from RNA-seq Data. *Non-Coding RNA* **3**, 8 (2017).
26. Gao, Y., Zhang, J. & Zhao, F. Circular RNA identification based on multiple seed matching. *Brief. Bioinform.* **19**, 803–810 (2018).
27. Memczak, S. *et al.* Circular RNAs are a large class of animal RNAs with regulatory potency. *Nature* **495**, 333–338 (2013).
28. Zhang, X.-O. *et al.* Diverse alternative back-splicing and alternative splicing landscape of circular RNAs. *Genome Res.* **26**, 1277–1287 (2016).
29. Li, H. Aligning sequence reads, clone sequences and assembly contigs with BWA-MEM. (2013).
30. Dobin, A. *et al.* STAR: ultrafast universal RNA-seq aligner. *Bioinformatics* **29**, 15–21 (2013).
31. Hoffmann, S. *et al.* A multi-split mapping algorithm for circular RNA, splicing, trans-splicing and fusion detection. *Genome Biol.* **15**, R34 (2014).
32. Kim, D. *et al.* TopHat2: accurate alignment of transcriptomes in the presence of insertions, deletions and gene fusions. *Genome Biol.* **14**, R36 (2013).
33. Cheng, J., Metge, F. & Dieterich, C. Specific identification and quantification of circular RNAs from sequencing data. *Bioinformatics* **32**, 1094–1096 (2016).
34. Westholm, J. O. *et al.* Genome-wide Analysis of Drosophila Circular RNAs Reveals Their Structural and Sequence Properties and Age-Dependent Neural Accumulation. *Cell Rep.* **9**, 1966–1980 (2014).
35. Hansen, T. B., Venø, M. T., Damgaard, C. K. & Kjems, J. Comparison of circular RNA prediction tools. *Nucleic Acids Res.* **44**, e58 (2016).
36. Hansen, T. B. Improved circRNA Identification by Combining Prediction Algorithms. *Front Cell Dev Biol* **6**, 20 (2018).
37. Peng, L. *et al.* Circular RNA ZNF609 functions as a competitive endogenous RNA to regulate AKT3 expression by sponging miR-150-5p in Hirschsprung's disease. *Oncotarget*, <https://doi.org/10.18632/oncotarget.13656> (2016).
38. Jeck, W. R. *et al.* Circular RNAs are abundant, conserved, and associated with ALU repeats. *RNA* **19**, 141–157 (2013).
39. Capel, B. *et al.* Circular transcripts of the testis-determining gene Sry in adult mouse testis. *Cell* **73**, 1019–1030 (1993).
40. Bachmayr-Heyda, A. *et al.* Correlation of circular RNA abundance with proliferation—exemplified with colorectal and ovarian cancer, idiopathic lung fibrosis, and normal human tissues. *Sci. Rep.* **5**, 8057 (2015).
41. Cobaleda, C., Schebesta, A., Delogu, A. & Busslinger, M. Pax5: the guardian of B cell identity and function. *Nat. Immunol.* **8**, 463–470 (2007).
42. Hystad, M. E. *et al.* Characterization of early stages of human B cell development by gene expression profiling. *J. Immunol.* **179**, 3662–3671 (2007).
43. Zheng, Q. *et al.* Circular RNA profiling reveals an abundant circHIPK3 that regulates cell growth by sponging multiple miRNAs. *Nat. Commun.* **7**, 11215 (2016).
44. Haferlach, T. *et al.* Clinical utility of microarray-based gene expression profiling in the diagnosis and subclassification of leukemia: report from the International Microarray Innovations in Leukemia Study Group. *J. Clin. Oncol.* **28**, 2529–2537 (2010).
45. Schotte, D. *et al.* MicroRNA characterize genetic diversity and drug resistance in pediatric acute lymphoblastic leukemia. *Haematologica* **96**, 703–711 (2011).
46. Yang, Y. *et al.* Novel Role of FBXW7 Circular RNA in Repressing Glioma Tumorigenesis. *J. Natl. Cancer Inst.* **110** (2018).
47. Qiu, L. *et al.* Circular RNA Signature in Hepatocellular Carcinoma. *J. Cancer* **10**, 3361–3372 (2019).
48. Adhikary, J. *et al.* Circular PVT1: an oncogenic non-coding RNA with emerging clinical importance. *J. Clin. Pathol.* **72**, 513–519 (2019).
49. Chen, J. *et al.* Circular RNA profile identifies circPVT1 as a proliferative factor and prognostic marker in gastric cancer. *Cancer Lett.* **388**, 208–219 (2017).
50. Ghafouri-Fard, S., Omrani, M. D. & Taheri, M. Long noncoding RNA PVT1: A highly dysregulated gene in malignancy. *J. Cell. Physiol.*, <https://doi.org/10.1002/jcp.29060> (2019).
51. Kun-Peng, Z., Xiao-Long, M. & Chun-Lin, Z. Overexpressed circPVT1, a potential new circular RNA biomarker, contributes to doxorubicin and cisplatin resistance of osteosarcoma cells by regulating ABCB1. *Int. J. Biol. Sci.* **14**, 321–330 (2018).
52. Tashiro, K., Tseng, Y.-Y., Konety, B. & Bagchi, A. MP99-18 Role of long non-coding RNA PVT1 in regulating MYC in human cancer. *Journal of Urology* **197** (2017).

53. Qin, S. *et al.* Circular RNA PVT1 acts as a competing endogenous RNA for miR-497 in promoting non-small cell lung cancer progression. *Biomed. Pharmacother.* **111**, 244–250 (2019).
54. Boldrin, E. *et al.* Expression and impact of miR-497-195 in pediatric ALL. *30. Jahrestagung der Kind-Philipp-Stiftung für pädiatrisch-onkologische Forschung*, <https://doi.org/10.1055/s-0037-1602219> (2017).
55. Yu, H., Chen, Y. & Jiang, P. Circular RNA HIPK3 exerts oncogenic properties through suppression of miR-124 in lung cancer. *Biochem. Biophys. Res. Commun.* **506**, 455–462 (2018).
56. Chen, G., Shi, Y., Liu, M. & Sun, J. circHIPK3 regulates cell proliferation and migration by sponging miR-124 and regulating AQP3 expression in hepatocellular carcinoma. *Cell Death Dis.* **9**, 175 (2018).
57. Kong, Y. *et al.* CircPLK1 sponges miR-296-5p to facilitate triple-negative breast cancer progression. *Epigenomics* **11**, 1163–1176 (2019).
58. Je, E. M., Yoo, N. J., Kim, Y. J., Kim, M. S. & Lee, S. H. Mutational analysis of splicing machinery genes SF3B1, U2AF1 and SRSF2 in myelodysplasia and other common tumors. *Int. J. Cancer* **133**, 260–265 (2013).
59. Langmead, B. & Salzberg, S. L. Fast gapped-read alignment with Bowtie 2. *Nat. Methods* **9**, 357–359 (2012).
60. Langmead, B., Trapnell, C., Pop, M. & Salzberg, S. L. Ultrafast and memory-efficient alignment of short DNA sequences to the human genome. *Genome Biol.* **10**, R25 (2009).
61. Bolger, A. M., Lohse, M. & Usadel, B. Trimmomatic: a flexible trimmer for Illumina sequence data. *Bioinformatics* **30**, 2114–2120 (2014).
62. Kim, D., Langmead, B. & Salzberg, S. L. HISAT: a fast spliced aligner with low memory requirements. *Nat. Methods* **12**, 357–360 (2015).
63. Love, M. I., Huber, W. & Anders, S. Moderated estimation of fold change and dispersion for RNA-seq data with DESeq. 2. *Genome Biol.* **15**, 550 (2014).
64. Chen, H. & Boutros, P. C. VennDiagram: a package for the generation of highly-customizable Venn and Euler diagrams in R. *BMC Bioinformatics* **12**, 35 (2011).
65. Meyer, L. H. *et al.* Early relapse in ALL is identified by time to leukemia in NOD/SCID mice and is characterized by a gene signature involving survival pathways. *Cancer Cell* **19**, 206–217 (2011).
66. Untergasser, A. *et al.* Primer3—new capabilities and interfaces. *Nucleic Acids Res.* **40**, e115 (2012).
67. Koressaar, T. & Remm, M. Enhancements and modifications of primer design program Primer3. *Bioinformatics* **23**, 1289–1291 (2007).
68. Andersen, C. L., Jensen, J. L. & Ørntoft, T. F. Normalization of Real-Time Quantitative Reverse Transcription-PCR Data: A Model-Based Variance Estimation Approach to Identify Genes Suited for Normalization, Applied to Bladder and Colon Cancer Data Sets. *Cancer Research* **64**, 5245–5250 (2004).
69. Betel, D., Koppal, A., Agius, P., Sander, C. & Leslie, C. Comprehensive modeling of microRNA targets predicts functional non-conserved and non-canonical sites. *Genome Biol.* **11**, R90 (2010).
70. Yu, H., Wang, J., Sheng, Q., Liu, Q. & Shyr, Y. beRBP: binding estimation for human RNA-binding proteins. *Nucleic Acids Res.* **47**, e26 (2019).
71. Hancock, J. M. & Bishop, M. J. ORF Finder (Open Reading Frame Finder). *Dictionary of Bioinformatics and Computational Biology*, <https://doi.org/10.1002/0471650129.dob0508> (2004).
72. Li, W. *et al.* Characterization of hsa_circ_0004277 as a New Biomarker for Acute Myeloid Leukemia via Circular RNA Profile and Bioinformatics Analysis. *Int. J. Mol. Sci.* **18** (2017).
73. Moore, S. J. *et al.* Fragile X syndrome with FMR1 and FMR2 deletion. *J. Med. Genet.* **36**, 565–566 (1999).
74. Meyer, C. *et al.* The MLL recombinome of acute leukemias in 2017. *Leukemia* **32**, 273–284 (2018).
75. Tsujimoto, Y., Cossman, J., Jaffe, E. & Croce, C. Involvement of the bcl-2 gene in human follicular lymphoma. *Science* **228**, 1440–1443 (1985).
76. Mullighan, C. G. *et al.* Rearrangement of CRLF2 in B-progenitor- and Down syndrome-associated acute lymphoblastic leukemia. *Nat. Genet.* **41**, 1243–1246 (2009).
77. Wang, G. *et al.* The effect of Hsa_circ_0001451 in clear cell renal cell carcinoma cells and its relationship with clinicopathological features. *J. Cancer* **9**, 3269–3277 (2018).
78. Ye, F. *et al.* circFBXW7 inhibits malignant progression by sponging miR-197-3p and encoding a 185aa protein in triple-negative breast cancer. *Molecular Therapy - Nucleic Acids*, <https://doi.org/10.1016/j.omtn.2019.07.023> (2019).
79. O’Neil, J. *et al.* FBW7 mutations in leukemic cells mediate NOTCH pathway activation and resistance to gamma-secretase inhibitors. *J. Exp. Med.* **204**, 1813–1824 (2007).
80. Enuka, Y. *et al.* Circular RNAs are long-lived and display only minimal early alterations in response to a growth factor. *Nucleic Acids Res.* **44**, 1370–1383 (2016).
81. Huret, J.-L. *et al.* Atlas of Genetics and Cytogenetics in Oncology and Haematology in 2013. *Nucleic Acids Res.* **41**, D920–D924 (2013).
82. Mullighan, C. G. *et al.* BCR-ABL1 lymphoblastic leukaemia is characterized by the deletion of Ikaros. *Nature* **453**, 110–114 (2008).
83. Viganò, E. *et al.* Somatic IL4R mutations in primary mediastinal large B-cell lymphoma lead to constitutive JAK-STAT signaling activation. *Blood* **131**, 2036–2046 (2018).
84. Lu, D., Luo, P., Wang, Q., Ye, Y. & Wang, B. Lu, D., Luo, P., Wang, Q., Ye, Y. & Wang, B. lncRNA PVT1 in cancer: A review and meta-analysis. *Clin. Chim. Acta* **474**, 1–7 (2017).
85. Yazdi, N. *et al.* Long noncoding RNA PVT1: potential oncogene in the development of acute lymphoblastic leukemia. *Turk. J. Biol.* **42**, 405–413 (2018).
86. Makishima, H. *et al.* Somatic SETBP1 mutations in myeloid malignancies. *Nature Genetics* **45**, 942–946 (2013).
87. Wang, J. *et al.* Circular RNA hsa_circ_0000567 can be used as a promising diagnostic biomarker for human colorectal cancer. *J. Clin. Lab. Anal.* **32**, e22379 (2018).
88. Xu, L. *et al.* CircSETD3 (Hsa_circ_0000567) acts as a sponge for microRNA-421 inhibiting hepatocellular carcinoma growth. *Journal of Experimental & Clinical Cancer Research* **38** (2019).
89. Abbas, S. *et al.* Integrated genome-wide genotyping and gene expression profiling reveals BCL11B as a putative oncogene in acute myeloid leukemia with 14q32 aberrations. *Haematologica* **99**, 848–857 (2014).
90. Czubak, K. *et al.* Global increase in circRNA levels in myotonic dystrophy. <https://doi.org/10.1101/489070>
91. Núñez-Enriquez, J. C. *et al.* Gene Expression Profiling of Acute Lymphoblastic Leukemia in Children with Very Early Relapse. *Arch. Med. Res.* **47**, 644–655 (2016).
92. Huang, Z. *et al.* Plasma Circular RNAs hsa_circ_0001953 and hsa_circ_0009024 as Diagnostic Biomarkers for Active Tuberculosis. *Frontiers in Microbiology* **9** (2018).

Acknowledgements

We acknowledge for financial support: AIRC (IG #20052 to SBo and GtK; MFAG #15674 to SBr); Department of Molecular Medicine, University of Padova (PRID 2017 to SBo); Cariparo (Pediatric research projects, GtK and SBo); International Graduate School of Molecular Medicine of Ulm University (to EB); Padova Institute of Paediatric Research (to AB and CF); German Research Foundation (SFB1074, B6 to LHM and KMD). EB is PhD student in co-tutelage with the Graduate school in Biosciences of the University of Padova.

Author Contributions

E.G., L.H.M., G.t.K. and S.B.o. conceived the study; E.B., A.B., S.B.r., L.T. and C.F. performed experiments; E.B. conducted the validations and screening in patients; E.G., A.D.M. and S.B.o. contributed bioinformatics methods and data analysis; L.H.M. and K.M.D. provided patient samples. E.G., E.B., G.t.K. and S.B.o. wrote the paper and made the figures. All authors revised the manuscript.

Additional Information

Supplementary information accompanies this paper at <https://doi.org/10.1038/s41598-019-50864-z>.

Competing Interests: The authors declare no competing interests.

Publisher's note Springer Nature remains neutral with regard to jurisdictional claims in published maps and institutional affiliations.



Open Access This article is licensed under a Creative Commons Attribution 4.0 International License, which permits use, sharing, adaptation, distribution and reproduction in any medium or format, as long as you give appropriate credit to the original author(s) and the source, provide a link to the Creative Commons license, and indicate if changes were made. The images or other third party material in this article are included in the article's Creative Commons license, unless indicated otherwise in a credit line to the material. If material is not included in the article's Creative Commons license and your intended use is not permitted by statutory regulation or exceeds the permitted use, you will need to obtain permission directly from the copyright holder. To view a copy of this license, visit <http://creativecommons.org/licenses/by/4.0/>.

© The Author(s) 2019